Metal particle seeding on urban surface samples

Emmanuel Kouakou Kouadio, Mathieu Goriaux, Philippe Laguionie, Véronique Ruban

Metal particle seeding on urban surface samples

Emmanuel Kouakou Kouadio, Mathieu Goriaux, Philippe Laguionie, Véronique Ruban
Environmental Science and Pollution Research (2022)
https://doi.org/10.1007/s11356-021-13789-7

Abstract

In order to estimate the resuspension of the particles empirically, it is necessary to carry out a homogeneous distribution of the particles on the tested surfaces. Thus, in many studies, seeding or deposition in experimental chambers is performed to quantify initial concentrations for subsequent resuspension experiments. The current study was carried out to assess metal particle seeding efficiency on four types of urban surfaces (slate, facade coating, tile, and glass) in a test chamber. To achieve this objective, we compared firstly different solubilization techniques of silver polydisperse particles (1.3–3.2 μm and 0.5–1.0 μm) and gold polydisperse particles (Ø<5 μm) for chemical quantification by ICP-MS. The result showed better yields in the case of gold for all solubilization techniques studied (82% ± 5% to 98% ± 2% for gold versus 23% ± 18% to 84% ± 12% for silver). Based on this result, four seeding tests were carried out with the gold particles (distribution in chamber centered on 1μm). The concentrations seeded on urban surfaces (mean ± SD) varied from 10,900 ± 1,900 $\mu g.m^{-2}$ (facade coating sample) to 1900 ± 390 $\mu g.m^{-2}$ (glass sample). The relative standard deviation of the measured concentrations equaled 9.5% (tested for aluminum foils), which was less than the measurement uncertainty of the recording equipment (≈14%) and reflected good seeding homogeneity. Observations by scanning electron microscopy coupled to microanalysis (SEM-EDX) were in agreement with these conclusions.

Introduction

Urban environments contain high concentrations of atmospheric metal particles due to their population density, types of activities, and the nature of their component surfaces (Laidlaw et al. 2012; Sternbeck et al. 2002; Thorpe and Harrison 2008). Such an environment is distinguished by both a high proportion of impervious surfaces and the specific nature of these surfaces (asphalt roads, glass, building uses). In their scientific expertise report on soil artificialization, Béchet et al. (2017) established the importance of taking surface composition into account for a full urban environment assessment (e.g., heat islands). They illustrated that the cumulative total of roofs and impermeable soils accounts for more than 50% of all surfaces in large cities (Bhatti and Tripathi 2014; Carlson and Sanchez-Azofeifa 1999; Li et al. 2011; Liu and Weng 2013). Many studies have been dedicated to the presence of metal particles in the air of cities (Sobhanardakani 2018, 2019). The metal elements identified, especially within residential areas, seem most often to display a distribution centered on a submicronic or fine fraction (Percot 2012). In addition, according to Allen et al. (2001), most metal particles in urban air are associated with an accumulation mode (i.e., of anthropogenic origin). Mbengue et al. (2014) compared the particle size distribution and chemical composition of airborne particles downwind of an urban industrial area at a site near Dunkirk (France) during winter 2012. Most elements measured (Sb, Cd, As, Mo, Pb, Zn, Cu, Ni, Cr, Mn, and V) were of anthropogenic origin. The authors found that, as opposed to coarse particles, the mass concentrations of submicron (PM_1) and ultrafine ($PM_{0.29}$) particles were higher downwind of the urban area. The mean concentration of metal elements measured was 1.7×10^3 $ng \cdot m^{-3}$. In other European cities, authors have measured, for example, 2.5×10^3 $ng \cdot m^{-3}$ in Augsburg, Germany (Gu et al. 2011), 783 $ng \cdot m^{-3}$ in Palermo, Italy (Dongarrà et al. 2010), 2.0×10^3 $ng \cdot m^{-3}$ in Zurich, Switzerland (Richard et al. 2011), and 200 $ng \cdot m^{-3}$ in London, UK (Visser et al. 2015). In Asia, Lyu et al. (2017) sampled metal particles, with aerodynamic diameters between 0.43 and 9 μm, present in Zhuzhou's (China) ambient air during a 2-month campaign. Measured trace element concentrations ranged from 10^{-2} to 10^4 $ng \cdot m^{-3}$, with Cu, Zn, As, Se, Ag, Cd, TI, and Pb all revealing a unimodal distribution in the fine particle size range (Ø < 2.1 μm).

In general, particle resuspension is not quantified in the current estimates of dry deposition and source identification (Lengweiler et al. 1998; Percot 2012). In cities, this phenomenon is mainly studied in the road traffic context (tire abrasion, road debris, sand particles) (Amato et al. 2012; Amato et al. 2016; Escrig et al. 2011; Ferm and Sjöberg 2015; Gehrig et al. 2010; Martuzevicius et al. 2011; Nicholson 1988; Sabin et al. 2006; Thorpe et al. 2007; Weinbruch et al. 2014). Resuspended particles are thus most often associated with the coarse mode (Damay 2010; Percot 2012). By failing to take resuspensions into account, the uses of such quantification in urban spaces can greatly overestimate the level of deposition. Several papers have reported that particle resuspension contributes significantly to the airborne emission of metals, such as zinc (Zn) and lead (Pb) (Damay 2010; Laschober et al. 2004; Percot 2012; Nicholson 1988; Nicholson 2009). However, resuspension remains a rather complex concept to accurately measure (Nicholson 2009). Various approaches have been developed to quantify resuspended elements. Generally speaking, particle resuspension is often expressed as either a resuspension factor K (in m^{-1}) or a resuspension rate Λ (in s^{-1}) (Nicholson 1988; Sehmel 1980). According to the authors, significant limitations constrain the application of these concepts under ambient conditions (Nicholson 1988; Sehmel 1980). The application of K or Λ requires an assessment of the deposit available for resuspension, i.e., the thickness of deposit suitable for resuspension (Nicholson 1993). In addition, it is difficult to determine the concentration of particles in the air directly above the considered surface; this concentration is used to calculate the resuspension factor or rate and depends on the height at which sampling is performed. For uniform areas (in terms of roughness height), the use of numerical models may be an option, but less so for highly heterogeneous environments like cities (Nicholson 1988). In practice, the application of K under actual conditions assumes that all airborne particles solely originate via the surfaces studied (Nicholson 1988). Emissions (whether natural or anthropogenic) then become difficult to separate from re-emitted elements.

Very few studies have been dedicated to resuspension without the use of K or Λ (Boor et al. 2013a, 2013b; Lengweiler et al. 1998). Lengweiler et al. (1998) studied the influence of various parameters on the deposition and resuspension tested simultaneously in a confined space. Their tests were carried out with talcum dust on painted wood fiber boards in the aim of evaluating the dust load, i.e., the amount of dust accumulated at the time of equilibrium between dust deposition ($g \cdot m^{-2} \cdot h^{-1}$) and resuspension ($g \cdot m^{-2} \cdot h^{-1}$). They concluded that, at least as far as the influence of turbulence is concerned, deposition and resuspension should be examined separately. Boor et al. (2013a, 2013b) developed two experimental chambers to study the aerodynamic resuspension of deposits of fluorescent particles on indoor environment surfaces. The first chamber was used to perform particle seeding on surface samples, while the second was used for resuspension tests under different wind speeds. Their approach refers to the term "absolute resuspension fraction" φ, which is defined as the change in seeding density following a windy episode. In short, whether encountering difficulties in applying the resuspension factor and rate in the field or implementing other approaches from the literature, it seems necessary to separately experiment with the two processes: the seeding (or deposition) phase and the seeded particle resuspension phase. Knowing the quantities of deposited particles assigned to the resuspension experiments would appear to be most critical. Hence, the experimental chambers are used for the particle seeding (or deposition) step on typical surfaces (Boor et al. 2013a, 2013b; Hussein et al. 2009a, 2009b; Ould-Dada and Baghini 2001; Thatcher et al. 1996; Qian and Ferro 2008). These chambers offer several advantages, including the choice of particle diameter and type of test surface. In most studies however, they have been built to test surfaces representative of indoor environments, e.g., offices or bedrooms (Byrne et al. 1995; Thatcher et al. 1996; Lai 2006; Hussein et al. 2009a, 2009b). Moreover, due to the type of particles being studied, the quantifications of particles seeded (or deposited) were essentially based on optical microscopy, fluorescence measurement, or weighing methods (Friess and Yadigaroglu 2001; Lengweiler et al. 1998; Matsusaka and Masuda 1996). During the experiments conducted by Lengweiler et al. (1998), the dust load was measured by vacuuming surface samples with a cleaning head on fiberglass filters. The amount of dust sampled was determined by differentiating the weight of the filter before and after sampling. In addition, because it was

difficult to recover small particles by suction, the authors relied on a sticky sheet to collect the particles from the surfaces, and the quantity of these particles was obtained by counting them under a microscope. In Boor et al. (2013a, 2013b), experimentation and quantification were carried out by means of stereomicroscopy combined with an image processing software. Nevertheless, this technique required working on very small test surfaces (i.e., 4.5 × 4.5 cm) and scanning the entire test surface during observation, or else assuming that the sampled particle distribution was perfectly uniform. All these conditions favor high measurement uncertainty, capable of influencing measurement of the part to be resuspended.

Finally, in his work, Fromentin (1989) indicates the importance of the effect of the homogeneity of the deposits (i.e., the different adhesion layers) on the resuspension flow. It seems that the conditions during aerosol deposition, i.e., during the first stage of the experiment, are key parameters for the resuspension process. Thus, a significant difference in the resuspension results was found as the inhomogeneity of the deposit increases (by two orders of magnitude over 10min). Thus, the effect of inhomogeneity has to be seriously taken into account; it influences the resuspension flow substantially. However, in most of the studies (Table 1), the question of deposit homogeneity (initial concentration in the case of resuspension experiments) is not or not clearly studied. In addition, measurement uncertainties related to the quantification techniques used are not mentioned (e.g., optical counting methods, fluorescence measurements or weighing….).

Table 1: Experimental conditions for studies involving particle seeding (or deposition) chambers

Authors	Installation	Particles tested	Diameter	Surfaces tested	Deposit quantification method	Surface loading (concentration)	Homogeneity estimation (RSD)
Braaten et al. (1988)	Wind tunnel: 2.33×7×7.62 cm	*Lycopodium* monolayer	28 µm	Glass	Optical system	Not specified	_
Fromentin (1989)	Tunnel: 25×25×350 cm	Multilayers of SnO_2 ; Fe_2O_3; Sn; Si	0.4–4.3 µm	Smooth stainless steel	Gravimetric weighing	100 to 1000 g·m^2	_
Braaten et al. (1990)	Wind tunnel: 1×1×2.5 m	Scattered monolayer of *Lycopodium*	27.8 µm	Glass (microscopic plate)	Optical system	Not specified	_
Wu and Russell (1992)	Wind tunnel: 1.0 m^2 × 9.0 m	Monolayer of uranine; polymer; *Lycopodium*; pollen	5–42 µm	Glass, plexiglass	Optical microscope, stereomicroscope, and camera	≈ 50–100 particles (for 24 cm^2)	_
Nicholson (1993)	Wind tunnel: 1×1×19.25 m	Silica spheres	4, 10, 18, and 22 µm	Concrete and grass substrates	Optical microscopy	Not specified	_
Braaten (1994)	Wind tunnel: 0,5×0,5×6 m	Ni; *Lycopodium*; glass beads; pollen	18–34 µm	Glass (microscopic plate)	Microscope	Not specified	_
Giess et al. (1994)	Perspex box: 80×50×75cm	Silica spheres	1, 5, and 10 µm	Grass (various heights)	Isokinetic sensor	40–100 µg·cm^{-2}	_
Thatcher and Layton (1995)	Two-storey house Total floor area: 230m^2	House dust (unseeded) in one home	0.3 to >25 µm	40% carpet and 60% hard floor	Optical particle-counting techniques	6–4340 µg·m^{-2}	_
Matsusaka and Masuda (1996)	Rectangular channel: 3×10×400 mm	Fly ash (and aggregates)	3 µm (10–30 µm)	Wall	Microscopy	Not specified	_
Thatcher et al. (1996)	Test chamber: 1.22×1.22×1.22 m	Solid ammonium fluorescein	0.1; 0.5; 0.7; 1.0; and 2.5 µm	Aluminum	Fluorometer	Not specified	_
Giess et al. (1997)	Perspex box	Silica spheres	1, 10, and 20 µm	Grass (various heights)	Isokinetic sensor	Not specified	_
Chiou and Tsai (2001)	Wind tunnel: 5×5×20 cm	Road dust	< 30 µm	Aluminum flat plate	Weighing	Not specified	_
Reeks and Hall (2001)	Tunnel: 5×0.2×0.2 m	Alumina spheres and graphite particles	12.2, 23, and 13 µm	Polished stainless steel	Photography	Not specified	_
Ould-Dada and Baghini (2001)	Test chamber: 80×50×65cm	Silica particles (with Dy [$Dy(NO_3)_3$] tracer)	1 µm	Spruce saplings	Weighing and instrumental neutron activation analysis	4.1 × 10^2 gDy·m^2	_
Buttner et al. (2002)	Experimental room	*Penicillium chrysogenum* spores	1.8–3.5 µm	Vinyl tile, loop pile, and cut-pile carpet	Microscope (counting CFUs)	10^6 and 10^7 CFU·m^2	_
Ibrahim et al. (2003)	Wind tunnel: 100×20.3×20.3 cm	Stainless steel spheres; glass spheres; *Lycopodium* spores	10–76 µm	Glass substrate	Camera	1 part·mm^{-2} (monolayer)	_

Ibrahim et al. (2004)	Wind tunnel: 1 m×20.3×20.3 cm	Stainless steel spheres	64–76 µm	Glass substrate	CCD camera	0.5–3 part·mm^{-2}	_
Lai and Nazaroff (2005)	Test chamber: 1.8 m^3	Solid ammonium fluorescein particles	0.9–9 µm	Aluminum oxide sandpapers	Fluorometer	Not specified	Carried out with copper foils: 15%
Lai (2006)	Test chamber: 1.8 m^3	Solid ammonium fluorescein particles	3.5;7.0, and 9.0 µm	Smooth glass plates, acetate sheets, and copper foil	Fluorometer	Not specified	carried out with copper foils: 15%
Ibrahim and Dunn (2006)	Wind tunnel: 1 m×20.3×20.3 cm	Stainless microspheres	64–76µm	Smooth glass substrates	CCD camera	≈ 0.5 part·mm^{-2}	_
Ibrahim et al. (2008)	Wind tunnel: 1 m×20.3cm ×20.3 cm	Soda lime glass microspheres	30.1; 52.6; 72.6; 90.3; and 111 µm	Glass substrate	CCD camera	< ~ 50 part·cm^{-2}	_
Qian et al. (2008)	Test house	Fluorescent polystyrene latex (seeded)	1 µm	Carpet	Microscope equipped with a fluorescent optical filter	4.30×10^8 part·m^{-2}	_
Qian and Ferro (2008)	Test chamber	ATD: Arizona test dust (seeded)	0.1–10 µm	Level-loop carpets and vinyl flooring	Weighing	20 g·m^{-2}	Particles deposit: 20% (mean value)
Rosati et al. (2008)	Test house and chamber	ATD (seeded)	0.5–20 µm	Medium-pile carpet	Scanning electron microscopy	221–2971 mg·m^{-2}	_
Hussein et al. (2009a, 2009b)	Test chamber: 1×1×1 m	NaCl (salt)	0.02–0.3 µm	Smooth aluminum surfaces	Fine particles: SMPS	Not specified	_
		Di-2-ethylhexyl-sebacate	0.5–8 µm		Coarse particles: APS		
Kassab et al. (2013)	Experimental duct: 180 cm long ×10 cm^2	Glass beads	Mean: 26.4 µm	Glass, ceramic, and hardwood substrates	Camera	≈ 4.31 part·mm^{-2}	_
			Mean: 36.2µm			≈ 3.60 part·mm^{-2}	_
			Mean: 45.31µm			≈ 1.94 part·mm–$^{-2}$	_
Boor et al. (2013b)	Experimental chamber: 0.05 m^3 and 0.08 m^3	Dyed, spherical polystyrene fluorescent particles	3 µm and 10 µm	Linoleum flooring and galvanized sheet metal	Fluorometric method	3.8–9.5 ×10^{-4} g·m^{-2}	_
		ATD	0 to 20 µm		Gravimetric methods	6.23–20.25 ×10^{-4} g·m^{-2}	_

This paper presents the first step of a general framework for quantifying the resuspension of metal particles under dry conditions (i.e., no rainfall) and in the urban outdoor environment. Since the resuspension phase requires homogeneous seeding and particles adapted to the ambient environment, a methodology for effective particle recovery and quantification is developed.

The main goals of the current investigation can be summarized as follows:

- To seed urban surfaces with $PM_{2.5}$ metal particles (micro-particles of silver (Ag) and gold (Au))
- To validate the choice of particle (analytical method)
- To develop a methodology for effective particle recovery and quantification by ICP-MS
- To evaluate the seedings obtained (homogeneity of concentrations by surface type)

Materials and methods

Description of the chamber

Seeding experiments were conducted in a 1 m^{-3} cubic lined plywood chamber. The plywood was chosen to minimize the effect of electrostatic charges between particles and chamber walls. Chamber sealing was ensured by cleats, a silicone gasket, and EPDM (ethylene propylene diene monomer) foam tape. The device is shown in Fig. 1 and was installed at the Water and Environment Laboratory (Gustave Eiffel University, Nantes); it consists of an air filter-drying system, a particle generator, and the chamber itself. Metal particles were generated using a 3-jet Collison nebulizer supplied with compressed air. In order to improve the quality of the compressed air supplied to the nebulizer, this air was dried and filtered by a filter-drying module. Three Festo MS4 pneumatic filters connected in series (5 µm, 1 µm, and 0.01 µm), associated with an MS4 membrane dehydrator, formed this filtration module. This serial system allowed for ultrafiltration and drying of the compressed air (residual particles < 0.1 µm, residual oil < 0.1 mg·m^{-3}). Two adjustable digital flowmeters (SMC flowmeter, model PFM7) were installed in the device, downstream of the filter-drying module. Each flowmeter provided an air flow rate of 10 L·min^{-1}: one injected the correct air flow into the nebulizer, while the other supplied dilution air for the input aerosols at the nebulizer outlet. Mixing and turbulent flow

were induced by a small 3000-rpm fan (12 V), mounted in the center of the ceiling 13.5 cm below the top. The characteristics and location of the fan were determined based on the work of Lai and Nazaroff (2005), who studied deposits of fluorescein particles. Most studies have introduced such devices to induce aerosol mixing and turbulence in the test chamber (Byrne et al. 1995; Lai and Nazaroff 2005; Hussein et al. 2009a, 2009b). However, no specific recommendations regarding fan speeds were found in the literature, given that chamber configurations and objectives differ from one author to another. System checkpoints were also monitored throughout our trials. A humidity, temperature, and pressure sensor was installed in the chamber during the entire seeding process; it was a KISTOCK KPA 320 automatic recorder. Moreover, a water bubbler connected to a low-flow suction pump (≈ 6.4 $L \cdot min^{-1}$) induced discharge from the system.

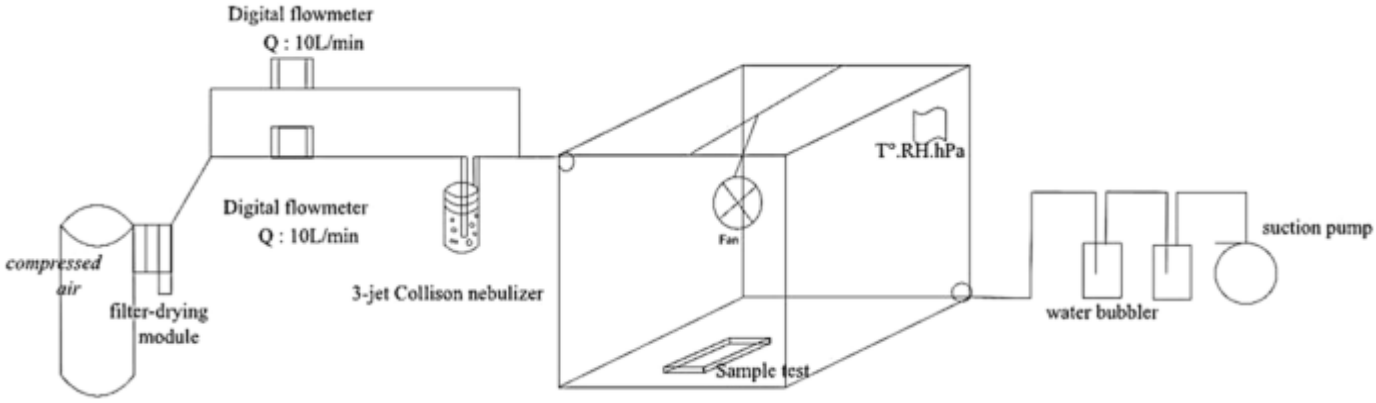

Fig. 1: Diagram of the seeding system used in these tests

In practice, each particle generation started by cleaning the chamber with compressed air (vacuum nebulizer). The optimal cleaning time was measured during preliminary tests using a GRIMM 1.108 particle counter; it was estimated at 60 min for a minimum pressure of 2 bars. The particle concentration in the nebulized solution equaled 20 $g \cdot L^{-1}$, and it remained limited to this quantity in order to comply with the manufacturer's specifications while generating a large mass of particles. The solution was a 50/50 mixture of ultrapure water and ethanol. Particle generation lasted 60 min, i.e., a time period corresponding to the aerosolization of approx. 20 mL of the mixture with a compressed air pressure of 3 bars. Once seeding had been completed, the suction was interrupted. The chamber was then sealed for 16 h, at the end of which it was opened, and the various seeded surfaces tested were covered with aluminum foil to facilitate their transport and avoid any lift-off.

Urban surface test sample arrangement during seeding

Four types of seeding surfaces were tested: slate, facade coating, tile (flat), and glass; all test samples were dimensioned 20 cm × 20 cm and selected on the basis of their representativeness in the urban environment. During testing, the samples were placed on the chamber floor. Byrne et al. (1995) determined the vertical (wall) and horizontal (floor) deposition fluxes in a test chamber for four aerosol particle size distributions (0.7 μm, 2.5 μm, 4.5 μm, and 5.4 μm). For each one, more than 50% of the generated material was deposited on the chamber floor. In practice, for our experiments, 16 test samples were deposited in the chamber during a given seeding test (4 surface samples per type of surface). As shown in Figs. 2 and 3, the test samples were arranged in two configuration modes, labeled 1 and 2. Mode 1 was a vertical line arrangement of four test samples of the same type (slate or facade coating or tile or glass). For mode 2, also arranged in a vertical line, test samples were alternated two-by-two according to their type. These arrangements were driven by technical choices. It was useful to seed as many different types of test samples as possible at the same time, in addition to assessing whether or not their location on the chamber floor significantly affected seeding homogeneity. The level of roughness by type of test piece had not been defined, so it was also considered to be

homogeneous over the entire surface for each test piece. Yet the test samples were identified by codes in order to identify any uniqueness in seeding results.

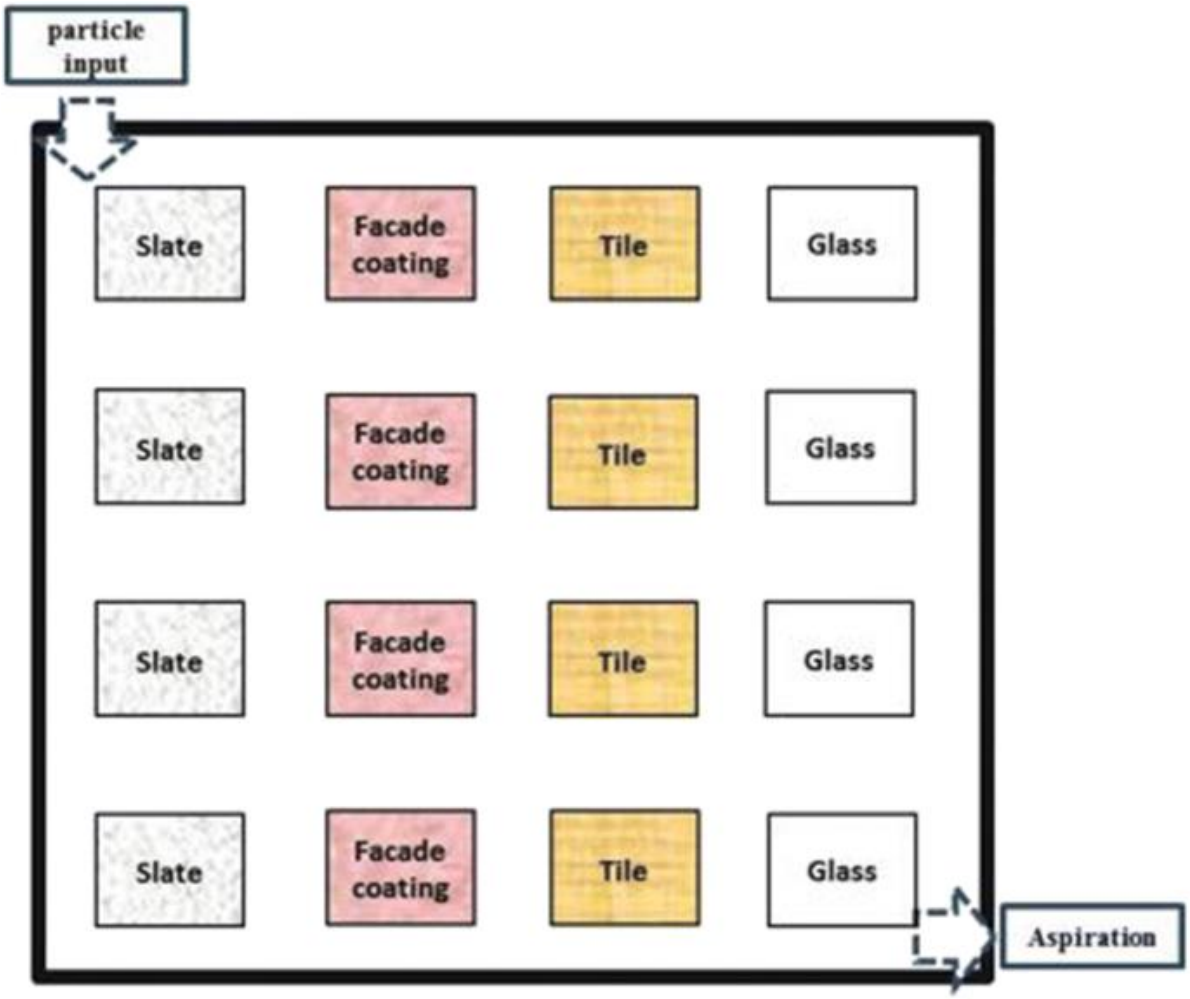

Fig. 2 : Arrangement of the test samples in the chamber - Mode 1

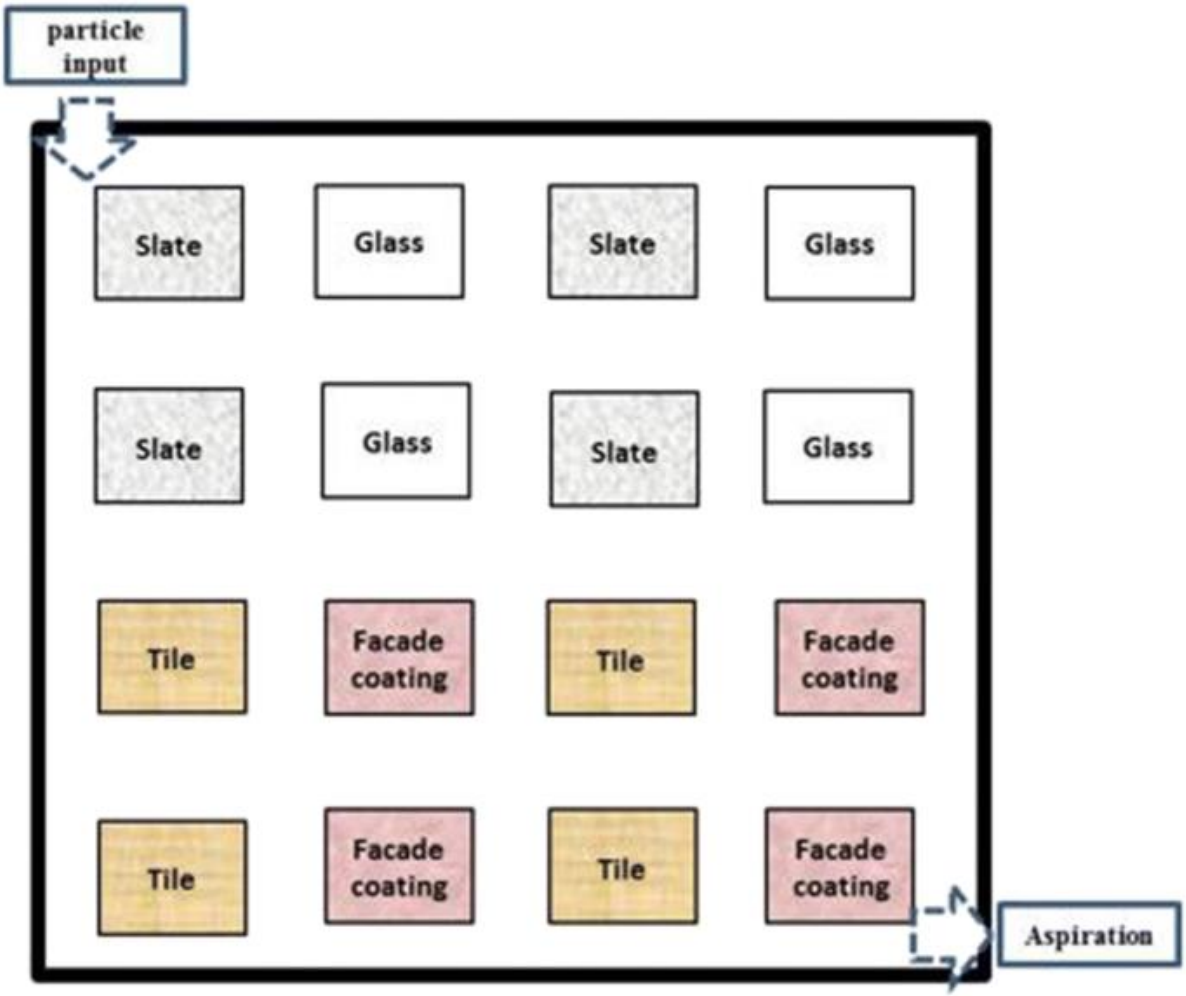

Fig. 3 : Arrangement of the test samples in the chamber - Mode 2

Particulate matter investigated

Selection of study particles

For subsequent ambient (outdoor) resuspension tests (subject to relative humidity, temperature, urban pollution, etc.), the abundance of the selected metals in urban ambient air flows had to be low, while their chemical stability needed to be at a good level. In addition, these metals had to differ from the elements being remobilized by test sample washing.

A blank wash was carried out to identify the chemical elements capable of being released from the test samples. The washing technique employed was identical to that applied during all experiments reported in this paper (see "Particle recovery after seeding"). Metals such as copper (Cu) and zinc (Zn) were present in high concentrations. Gold and silver were selected for further work based on the blank results (zero/low concentration in the test sample blanks). Gold (Au) was selected for both its low abundance in ambient air and chemical stability. Silver (Ag) was selected for its very low concentrations (close to the limit of quantitation) measured in the blanks. Both are transition metals; they are not highly reactive with water at ambient temperature. The test particles (Ag and Au) were spherical and 99.9% pure polydisperse powder (Alfa Aesar/ThermoFischer). A logistical limit was imposed on the use of metal micro-particles as we were unable to find monodisperse size powders on the market. The ranges supplied by the distributor and used in this study were thus powders with diameters varying between 1.3–3.2 and 0.5–1.0 μm for silver and a powder with diameters smaller than 5 μm for gold. The size distribution of the particles generated in the chamber during seeding was centered on 1 μm (particle counter MINI-WRAS 1371, GRIMM).

Effectiveness of analytical methods associated with the selected particles

In order to be quantified by means of ICP-MS (inductively coupled plasma mass spectrometry), the metals had to be solubilized. After selecting the test metals, the first operation consisted of evaluating the solubilization efficiency of each particle type as well as the efficiency of their quantification by ICP-MS (8900 Triple Quadrupole). All methods tested were based on LEE's internal protocols for the dissolution of metals present in all types of water (as adapted from Standard NF EN ISO 11885 (2009)). To determine the most effective method, yields were deduced for each type of particle according to the method applied. Solubilization was performed on volumes of acidified ultrapure water (pH=1, HNO_3: nitric acid) doped with silver or gold particles. The concentration of the doped solutions was 200 $\mu g \cdot L^{-1}$ regardless of the element. This concentration corresponded to the highest point on the ICP-MS calibration curve. The mixtures were mechanically homogenized before sampling. Two analytical methods were compared: metal particle solubilization in total fractions and solubilization in extractable fractions. The total fraction is the sum of both the dissolved and particulate fractions. The dissolved/particulate separation was achieved by membrane filtration (MF-Millipore, pore diameter: 0.45 μm). Subsequently, dissolved fractions were directly analyzed by ICP-MS; also, particulate fractions, referred to here as "filters" (filters = MF-Millipore membrane + particles Ø > 0.45 μm), were mineralized for measurement by ICP-MS as well. The filters were mineralized in various ways, depending on the nature of the tested particles. In the case of silver particles, two mineralization processes were performed, namely, total hydrofluoric and perchloric acid attacks and hot filter mineralization with concentrated nitric acid. The gold filters were exclusively mineralized using the hot acid mineralization process, which was performed with *aqua regia*. The metals in the extractable fractions were solubilized directly on the doped samples, without separating out the dissolved and particulate fractions. The solutions were thus acidified (HNO_3 for silver and *aqua regia* for gold) and then evaporated. The residues obtained after evaporation were once again recovered, with the various acids and ultrapure water, and heated for 1 h. The preparations were ultimately diluted with ultrapure water before conducting the ICP-MS measurements.

Particle recovery after seeding

A washing method was developed as part of this study to recover the seeded particles from test samples. Various authors have used washing techniques to estimate the quantity of particles deposited on test surfaces (Maro et al. 2008; Percot 2012; Roupsard 2013). After seeding, each test sample was therefore washed with 600 mL of an ultrapure water solution acidified to pH=1 with nitric acid. Washings took place in polyethylene tanks using a laboratory wash bottle. This technique was the same for all test samples: 500 mL of washing solution was introduced to thoroughly rinse the test sample and then 100 mL to rinse the tray and recover any residual particles. The acidity (pH=1) of the wash solution allowed for chemical stabilization of the recovered solutions while maintaining test sample structural integrity throughout the testing campaign. Particle concentrations measured as a result of washing were correlated with the test sample surface area ($\mu g \cdot m^{-2}$).

One of the main objectives of the washing technique developed was to achieve efficient recovery (i.e., recovering a maximum quantity of seeded particles, saving time and limiting the volume of solution used). Based on previous studies (Maro et al. 2008; Roupsard 2013), we estimated that washing as is would not have been effective in relying on a single operation. Therefore, in order to carry out just a single washing operation without underestimating the exact seeded concentrations, experimental correction factors were defined. For this purpose, a preliminary test of successive washes was run on the test samples until obtaining concentrations close to or below the ICP-MS limit of quantification. Four washes (4 × 600 mL of wash solution) were necessary to reach these values. This test was conducted after validating the study particles and analytical method. We were able to establish experimental correction factors for each type of test sample when only one washing operation was performed.

Results and discussion

Particles investigated

Silver particles

Table 2 shows the yields obtained for silver particles by the various solubilization methods employed. Regardless of size range and method, average yields were all below 50%, except for hot mineralization in the 0.5–1.0 µm range, where the values equaled 51% and 84% for extractable and total fractions, respectively. The low yields observed could be due to silver sorption phenomena on the containers used for sample preparation (polyethylene tubes). They might also be due to the chemical stability of silver in the doped samples before solubilization. We could not explain the best yields being obtained for the 0.5–1.0 µm range; however, even though these yields are higher than the others, they still all lie below 90%. In addition, the silver particles tested seem to resist remaining in suspension in the doped solutions as thin films of particles, especially silver, were observed on the sample surface. We concluded that, in our study context, silver particles were not adequate for future resuspension experiments. The difficulty involved in avoiding particle losses during pretreatment (sorption, particle film, or other phenomena) and associated errors could strongly influence resuspension quantification.

Table 2 : Yields of the various silver particle solubilization methods

Extractable fraction (no separation of dissolved/particulate fractions)		
Particle diameter (Ag)	Mean yield	RSD
Ø: 1.3–3.2 µm	48%	22%
Ø: 0.5–1.0 µm	51%	32%
Total fraction (dissolved + filters by hot mineralization)		
Particle diameter (Ag)	Mean yield	RSD
Ø: 1.3–3.2 µm	48%	2%
Ø: 0.5–1.0 µm	84%	12%
Total fraction (dissolved + filters by total attack)		
Particle diameter (Ag)	Mean yield	RSD
Ø: 1.3–3.2 µm	23%	18%
Ø: 0.5–1.0 µm	44%	14%

Gold particles

Table 3 presents the yields resulting from the various gold solubilization methods. The concentrations measured in the dissolved and particulate fractions (hot mineralization) have an average yield of 82% ± 5%; this figure was 98% ± 2% for the extractable fraction method. The solubilization of gold in the extractable fraction had yielded nearly twice as much as all methods applied to silver particles. The relative standard deviations of these measurements were smaller for the tests with gold particles than those with silver (2% to 5% for gold, 2% to 32% for silver).

Table 3 : Yields of the various gold particle solubilization methods

Extractable fraction (no separation of dissolved/particulate fractions)		
Particle diameter (Au)	Mean yield	RSD
Ø < 5 µm	98%	2%
Total fraction (dissolved + filters by hot mineralization)		
Particle diameter (Au)	Mean yield	RSD
Ø < 5 µm	82%	5%

On the basis of these results, gold particles were accepted as model particles for the next step. The gold solubilization method in the extractable fraction was selected as the most appropriate pretreatment method for analysis of these particles according to ICP-MS. In addition, the chemical stability of gold (in both air and water) will provide a great advantage during outdoor resuspension testing. Table 4 presents the experimental correction factors obtained for 3 successive washings of the test samples (recovery of gold particles). A 4th washing was also performed. The recovery rates were not taken into account due to the low concentration values obtained after measurement (i.e., concentrations below or equal to the ICP-MS limit of quantification). In the remainder of this work, these factors were applied to the concentrations measured on urban surface samples after each gold particle seeding test.

Table 4 : Experimental correction factors obtained for gold particles

Surface sample type	Experimental correction factor
Slate	1.14
Facade coating	1.07
Tile	1.26
Glass	1.02

Quantification of seeded gold particle concentrations

Seeding conditions

The pressure values measured within the chamber during testing ranged from 995 to 1039 hPa. The average temperatures measured, between 19 and 21°C, were close to those of the ambient environment (± 1°C). The relative humidity (RH) observed throughout the tests varied from 42 to 64% with a mean of 53%; it was important to ensure this value remained below 67% (Kim et al. 2010). An RH below this threshold makes it possible to neglect the particle-surface capillary forces (Kim et al. 2010), which are suspected to influence the resuspension phenomenon. Scanning electron microscopy (SEM, model Hitachi SU5000, combined with an EDX-Xflash Brucker detector) observations were also carried out on both carbon scotch pieces (Ø = 6 mm) and small slate test samples (Ø ≈ 10 mm). The objective of this observation was to verify the conformity of the particle sizes indicated by the supplier and their distribution on the surfaces (homogeneity, possible aggregate formation, monolayer or multilayer condition). The carbon scotch and slate samples were placed at different points in the chamber and seeded with gold particles. The particles observed by SEM and the sizes were indeed well within the range indicated by the supplier. The gold particles on both the carbon scotch and slate samples were individually and rather homogeneously distributed over the observed surfaces. The seeding was monolayer, and no aggregates could be observed.

Seeding homogeneity and measured concentrations

In order to evaluate the robustness of the homogeneity of gold particle seeding, an experiment was conducted with aluminum foil. Nine aluminum squares approximately 20 cm × 20 cm (equal to a test sample area) were distributed on the test chamber floor. The quantities of gold seeded were measured for each foil (with replicates). The relative standard deviation of the measured concentrations equaled 9.5%; this value was less than the ICP-MS measurement uncertainty (≈14%). This result allowed concluding that gold particles were homogeneously distributed over the various points of the chamber floor during seeding tests. In their work with fluorescein particles, Lai and Nazaroff (2005) obtained a maximum relative difference of less than 15% among the various points in their chamber. Their tests were performed on eight 2 cm × 2 cm copper sheets, and they concluded that for this standard deviation (SD < 15%), the concentration in the chamber was assumed to be “reasonably” uniform. Four gold seeding tests were performed on the surface test samples. Figures 4, 5, 6, and 7 show the mean surface concentrations from these tests (tests 1 and 2: mode 1 configuration; tests 3 and 4: mode 2 configuration). The average (mean ± SD) maximum and minimum concentrations measured

across all tests were 10,900 $\mu g \cdot m^{-2}$ (facade coating, test 2) and 1900 $\mu g \cdot m^{-2}$ (glass, test 3). For test 1, the mean concentrations by test sample type were 6200 ± 900 $\mu g \cdot m^{-2}$, 9000 ± 1000 $\mu g \cdot m^{-2}$, 3800 ± 500 $\mu g \cdot m^{-2}$, and 7400 ± 1000 $\mu g \cdot m^{-2}$, for slate, facade coating, tile and glass, respectively. Measurements during tests 2, 3, and 4 reported 4847 ± 679 $\mu g \cdot m^{-2}$, 4930 ± 690 $\mu g \cdot m^{-2}$, and 3152 ± 441 $\mu g \cdot m^{-2}$ on the slate; 7700 ± 1100 $\mu g \cdot m^{-2}$, 3900 ± 500 $\mu g \cdot m^{-2}$, and 4300 ± 600 $\mu g \cdot m^{-2}$ on façade coating; 7700 ± 1100 $\mu g \cdot m^{-2}$, 4000 ± 600 $\mu g \cdot m^{-2}$, and 5400 ± 800 $\mu g \cdot m^{-2}$ on tile; and 5900 ± 800 $\mu g \cdot m^{-2}$, 2800 ± 400 $\mu g \cdot m^{-2}$, and 3500 ± 500 $\mu g \cdot m^{-2}$ on glass. As these figures attest, the concentration values within each test are of the same order of magnitude for each type of surface. Nevertheless, a decrease in the quantities measured between test 1 and the other tests is noticeable. We have attributed this decline to the nebulizer. A gradual clogging of the probe spray nozzle orifices would have occurred over time, leading to a reduction in the quantity of particles generated in the chamber and thus received on the surfaces.

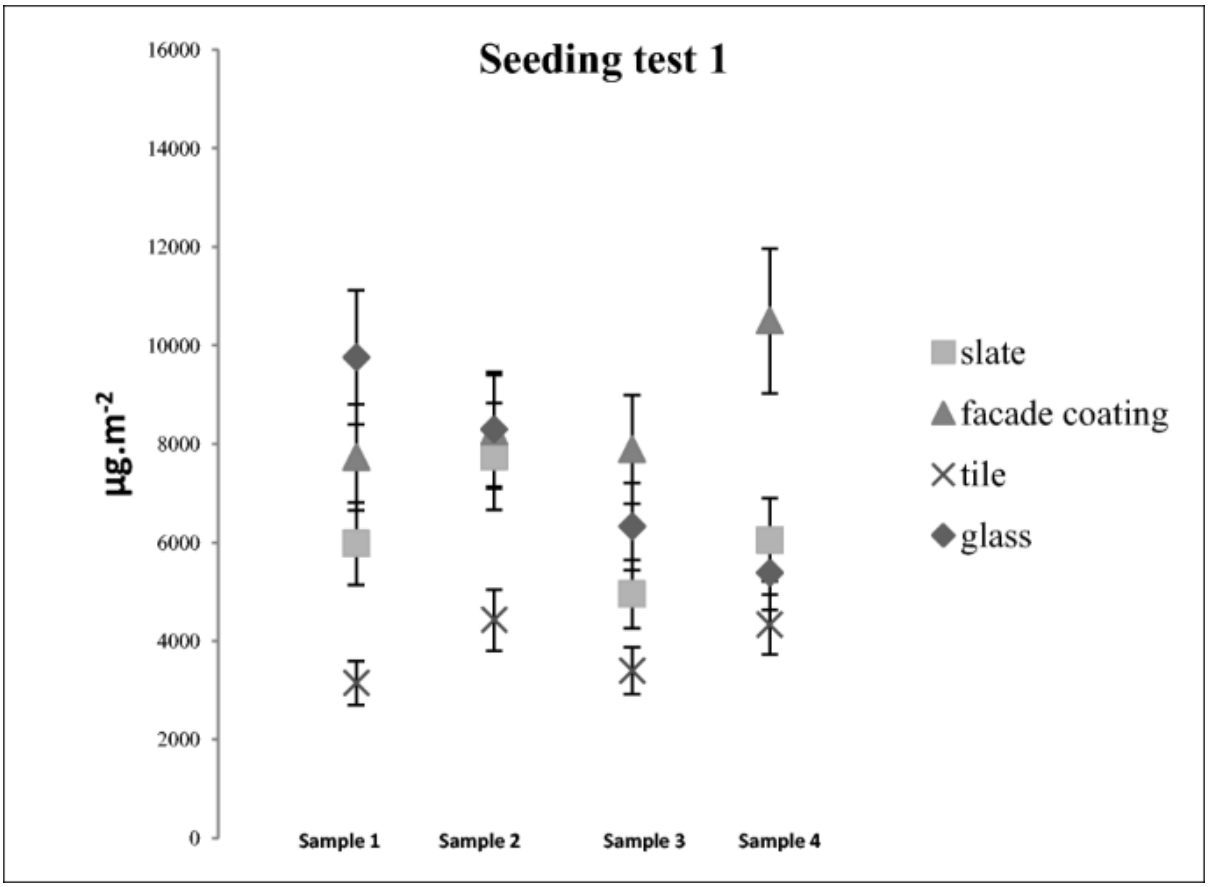

Fig. 4 : Gold particle concentrations measured for seeding test 1

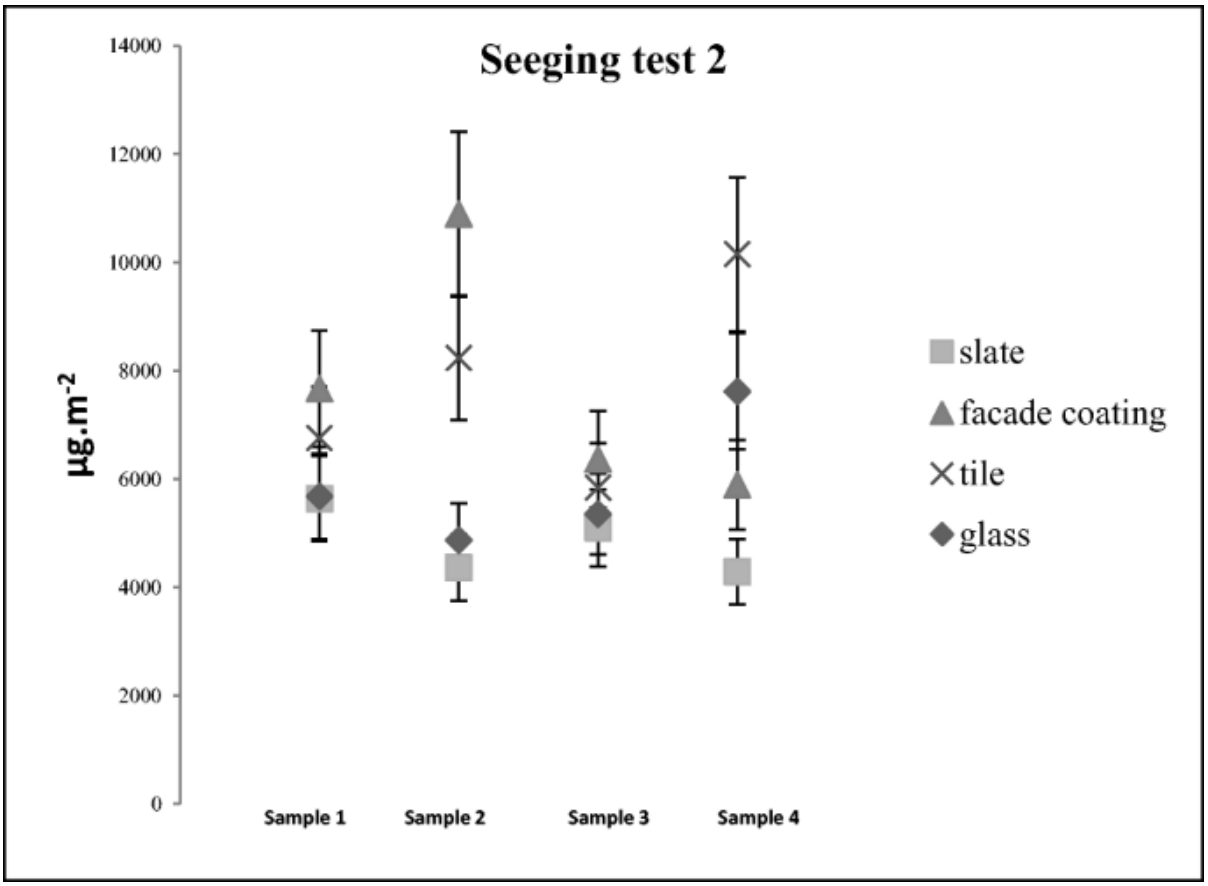

Fig. 5: Gold particle concentrations measured for seeding test 2

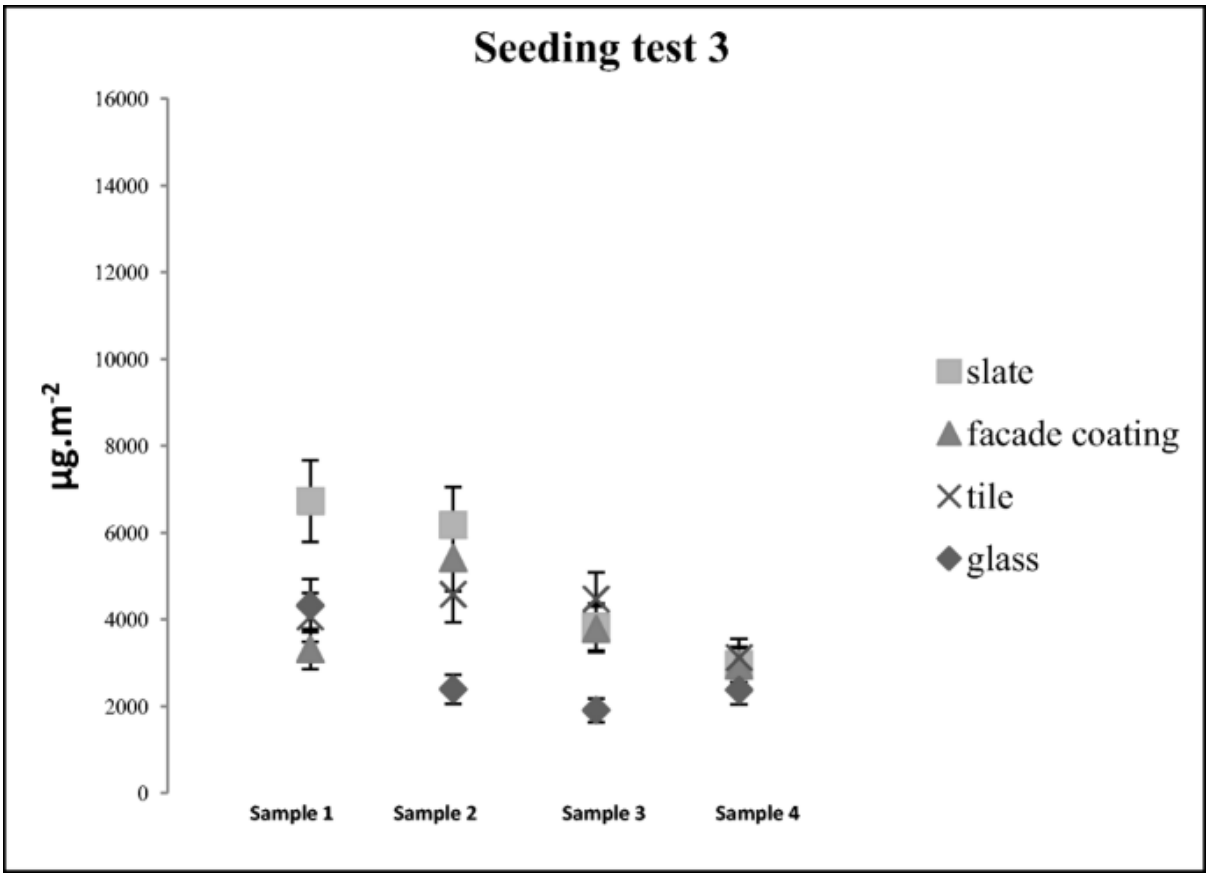

Fig. 6 : Gold particle concentrations measured for seeding test 3

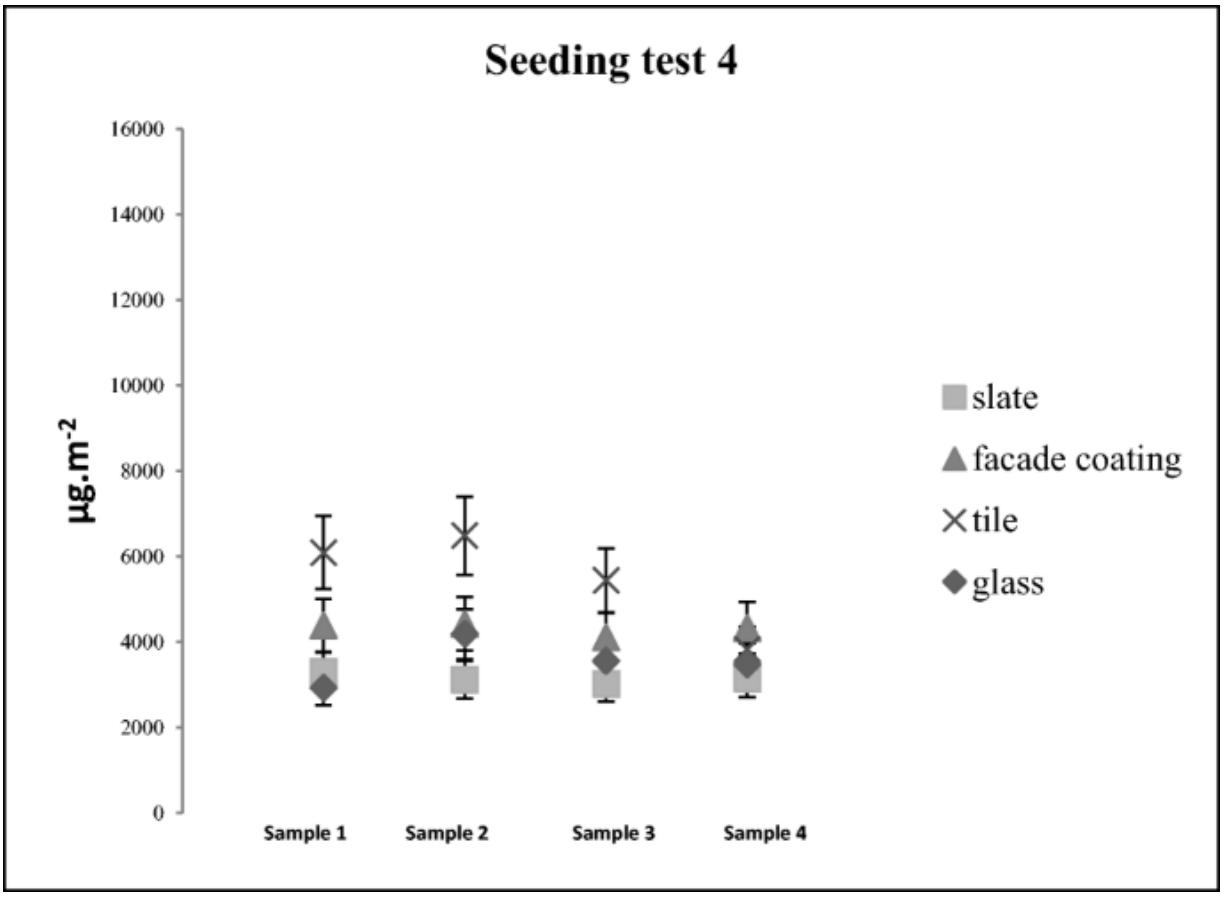

Fig. 7 : Gold particle concentrations measured for seeding test 4

Table 5 summarizes the relative standard deviations derived from the measured gold concentrations; the test sample values ranged from 3 to 32% for slate, 3 to 13% for facade coating, 15 to 21% for tile, and 13 to 34% for glass. However, these deviations did include the ICP-MS measurement uncertainty, which at the time of testing was ≈14%. Except for slight variations in temperature, humidity, and pressure within the chamber, all test parameters remained unchanged. No real constant is observed in the deviation values. With regard to the impact of clogging, it was found that the data from test 1 (before nebulizer clogging) varied from 13 to 23%, with the largest differences being observed for test 3. In test 4, a reduction in the deviations can be observed. Prior to this test (test 4), the nebulizer had been unclogged using ultrasound. Thus, test 1 was carried out before the clogging and test 4 after the unclogging procedure. Tests 2 and 3, on the other hand, were carried out, while the nebulizer was clogging. Even without taking into account the impact of nebulizer clogging, the differences obtained lie within the ranges found in the literature.

Table 5 : Relative standard deviations deduced from the seeding tests

Surface sample type	RSD			
	Test 1	Test 2	Test 3	Test 4
Slate	16%	11%	32%	3%
Facade coating	13%	25%	24%	3%
Tile	15%	21%	21%	19%
Glass	23%	18%	34%	13%

As shown in Table 6, in the literature, only Lai and Nazaroff (2005) and Qian and Ferro (2008) have clearly estimated the homogeneity of seeding on the surface. The coefficients of variation between seedings (for the same type of surface) were 15% (preliminary test on copper foil) and 20%, respectively. Qian and Ferro (2008) also performed a homogeneity check in the chamber using sulfur hexafluoride (SF6) at six different locations in the chamber. The conclusions obtained with this gas were not in agreement with the estimates made directly from the deposits. The differences in concentrations between a control point and the other 5 points ranged from

−7 ± 4 to 43 ± 12%. It therefore appears that the verification technique plays an important role in the validation of homogeneity. This indicates the interest of carrying out these homogeneity tests as close as possible to the method used for deposition (same type of particle, for example). It can be assumed that the assessments carried out directly from the deposits present results closer to reality. In Table 6, we have also estimated the coefficients of variation from the results presented by different authors. For example, in the work of Rosati et al. (2008), these estimated coefficients varied from 6 to 44%, while in the case of Kassab et al. (2013), they varied from 33 to 43%. Boor et al. (2013b) worked with 3µm and 10µm spherical polystyrene particle monolayer deposits (d = 1060 kg·m^{-3}) for resuspension testing; they obtained seeding densities of 67 ± 19 particles/mm^2 and 0.73 ± 0.16 particles/mm^2, respectively. For these values, the RSD correspond to 28% of the measured quantities for the 3 µm diameters and 22% for the 10µm diameters. Their seeding was carried out on test surfaces twenty times smaller than those of our tests, and their seeded particles were quantified by optical measurement. Compared to the results of Boor et al. (2013a, 2013b), due to the size of the surfaces tested in our study (nearly 20 times larger), our deviations can be considered an improvement. Moreover, compared to optical counting, a chemical method should ensure greater robustness in the quantification of deposits. The relative standard deviations of our measurements lie above the 9.5% obtained with aluminum foil; however, it is important to note that the test sample roughness was not measured. Hypotheses formulated during the experimental set-up suggested neglecting the potential impact of this parameter. For one thing, the roughness was considered uniform over the entire test sample surface. Also, the urban surface test samples used in this work, similar to those encountered in actual urban environments, could hardly observe such uniformity. Lastly, the roughness was considered to be identical, e.g., between two test samples of the same type. These assumptions could explain the higher relative standard deviation values than those observed for aluminum foil.

Table 6 : Comparison of deposit homogeneity in the literature

Authors	Particles tested	Diameter	Surfaces tested	Deposit quantification method	surface loading (concentration)	Homogeneity estimation (RSD)
Lai and Nazaroff (2005)	Solid ammonium fluorescein	0.9–9 µm	Aluminum oxide sandpapers	Fluorometer	Not specified	Carried out with copper foils: 15%
Qian and Ferro (2008)	ATD (Arizona test dust)	0.1–10 µm	New and old level-loop carpets, and vinyl flooring	Weighing	20 g·m^{-2}	20% of the mean value Test with sulfur hexafluoride (SF6) at six different locations in the chamber: 43%, 14%, 10%, −7%, and 26%
Rosati et al. (2008)	ATD	0.5–20 µm	Medium-pile carpet	Scanning electron microscopy	221–2971 mg·m^{-2}	6 to 44% (estimated)
Kassab et al. (2013)	Glass beads	Mean: 26.41µm	Glass, ceramic, and hardwood substrates	Camera	≈ 4.31±1.70 part·mm^{-2}	39% (estimated)
		Mean: 36.24µm			≈ 3.60±1.53 part·mm^{-2}	43% (estimated)
		Mean: 45.31µm			≈ 1.94±0.64 part·mm^{-2}	33% (estimated)
Boor et al. (2013b)	Dyed, spherical polystyrene fluorescent	3 µm and 10 µm	Linoleum flooring and galvanized sheet metal	Fluorometric method	3 µm : 9.5 ± 2.7×10^{-4} g·m^{-2} 10 µm: 3.8 ± 0.84×10^{-4} g·m^{-2}	28% (estimated) 22% (estimated)
	ATD	0 to 20 µm		Gravimetric methods	1–20 µm: 6.23 ± 1.10 to 20.25 ± 1.91 g·m^{-2}	9 to 25% (estimated)

Conclusions

Apart from experiments conducted in a chamber or wind tunnel, characterizing the resuspension of particles in an outdoor environment can be very complex. The objective of this paper was to evaluate the seeding step of metal micro-particles on urban surface samples intended for resuspension tests. An experimental approach was developed involving a seeding chamber along with a methodology for recovering and quantifying the deposited materials. This study is original by virtue of using metal particles for the seeding. Results showed that for our experimental context, gold particles are the most suitable, for analytical reasons, for both seeding and future resuspension work in urban outdoor environments. The test chamber made it possible to carry out monolayer seeding of individual gold micro-particles on urban surface

samples. The relative standard deviations of concentrations among surface samples ranged from 3 to 34%. The originality of this method prevented drawing any comparisons with previous works. However, the results obtained with aluminum foils, to account for homogeneous roughness (RSD = 9.5%), did show the robustness of particle seeding homogeneity in our chamber. As a matter of fact, this difference was smaller than that found in the literature; future adjustments will aim to reduce it even further.

Availability of data and materials

The datasets used and/or analyzed during the current study are available from the corresponding author on reasonable request.

References

Allen AG, Nemitz E, Shi JP, Harrison RM, Greenwood JC (2001) Size distributions of trace metals in atmospheric aerosols in the United Kingdom. Atmos Environ 35(27):4581–4591. https://doi.org/10.1016/S1352-2310(01)00190-X

Amato F, Schaap M, van der Gon HACD, Pandolfi M, Alastuey A, Keuken M, Querol X (2012) Effect of rain events on the mobility of road dust load in two Dutch and Spanish roads. Atmos Environ 62:352–358. https://doi.org/10.1016/j.atmosenv.2012.08.042

Amato F, Favez O, Pandolfi M, Alastuey A, Querol X, Moukhtar S, Bruge B, Verlhac S, Orza JAG, Bonnaire N, le Priol T, Petit JF, Sciare J (2016) Traffic induced particle resuspension in Paris: emission factors and source contributions. Atmos Environ 129:114–124. https://doi.org/10.1016/j.atmosenv.2016.01.022

Béchet B, Le Bissonnais Y, Ruas A, Aguilera A, André M, et al. (2017) Sols artificialisés et processus d'artificialisation des sols, Déterminants, impacts et leviers d'action. INRA (France), pp. 609. hal-01687919

Bhatti SS, Tripathi NK (2014) Built-up area extraction using Landsat 8 OLI imagery. GISci Remote Sens 51(4):445–467. https://doi.org/10.1080/15481603.2014.939539

Boor BE, Siegel JA, Novoselac A (2013a) Monolayer and multilayer particle deposits on hard surfaces: literature review and implications for particle resuspension in the indoor environment. Aerosol Sci Technol 47(8):831–847. https://doi.org/10.1080/02786826.2013.794928

Boor BE, Siegel JA, Novoselac A (2013b) Wind tunnel study on aerodynamic particle resuspension from monolayer and multilayer deposits on linoleum flooring and galvanized sheet metal. Aerosol Sci Technol 47(8):848–857. https://doi.org/10.1080/02786826.2013.794929

Braaten DA (1994) Wind tunnel experiments of large particle reentrainment-deposition and development of large particle scaling parameters. Aerosol Sci Technol 21(2):157–169. https://doi.org/10.1080/02786829408959705

Braaten DA, Paw KTU, Shaw RH (1988) Coherent turbulent structures and particle detachment in boundary layer flows. J Aerosol Sci 19(7):1183–1186. https://doi.org/10.1016/0021-8502(88)90131-0

Braaten DA, Paw KTU, Shaw RH (1990) Particle resuspension in a turbulent boundary layer-observed and modeled. J Aerosol Sci 21(5):613–628. https://doi.org/10.1016/0021-8502(90)90117-G

Buttner MP, Cruz-Perez P, Stetzenbach LD, Garrett PJ, Luedtke AE (2002) Measurement of airborne fungal spore dispersal from three types of flooring materials. Aerobiologia 18(1):1–11. https://doi.org/10.1023/A:1014977900352

Byrne MA, Goddard AJH, Lange C, Roed J (1995) Stable tracer aerosol deposition measurements in a test chamber. J Aerosol Sci 26(4):645–653. https://doi.org/10.1016/0021-8502(95)00003-U

Carlson TN, Sanchez-Azofeifa GA (1999) Satellite remote sensing of land use changes in and around San Jose, Costa Rica. Remote Sens Environ 70:247–256. https://doi.org/10.1016/S0034-4257(99)00018-8

Chiou SF, Tsai CJ (2001) Measurement of emission factor of road dust in a wind tunnel. Powder Technol 118(1–2):10–15. https://doi.org/10.1016/S0032-5910(01)00289-3

Damay P (2010) Détermination expérimentale de la vitesse de dépôt sec des aérosols submicroniques en milieu naturel: influence de la granulométrie, des paramètres micrométéorologiques et du couvert INSA de Rouen. Français. NNT: 2010ISAM0020. tel-00558201

Dongarrà G, Manno E, Varrica D, Lombardo M, Vultaggio M (2010) Study on ambient concentrations of PM10, PM10-2.5, PM2.5 and gaseous pollutants. Trace Elements and Chemical Speciation of Atmospheric Particulates. Atmos Environ 44(39):5244–5257. https://doi.org/10.1016/j.atmosenv.2010.08.041

Escrig A, Amato F, Pandolfi M, Monfort E, Querol X, Celades I, Sanfélix V, Alastuey A, Orza JAG (2011) simple estimates of vehicle-induced resuspension rates. J Environ Manag 92(10):2855–2859. https://doi.org/10.1016/j.jenvman.2011.06.042

Ferm M, Sjöberg K (2015) Concentrations and emission factors for PM2.5 and PM10 from Road Traffic in Sweden. Atmos Environ 119:211–219. https://doi.org/10.1016/j.atmosenv.2015.08.037

Friess H, Yadigaroglu G (2001) A generic model for the resuspension of multilayer aerosol deposits by turbulent flow. Nucl Sci Eng 138(2):161–176. https://doi.org/10.13182/NSE01-A2207

Fromentin A (1989) Particle resuspension from a multi-layer deposit by turbulent flow PSI (38): Switzerland

Gehrig R, Zeyer K, Bukowiecki N, Lienemann P, Poulikakos LD, Furger M, Buchmann B (2010) Mobile load simulators - a tool to distinguish between the emissions due to abrasion and resuspension of PM10 from Road Surfaces. Atmos Environ 44(38):4937–4943. https://doi.org/10.1016/j.atmosenv.2010.08.020

Giess P, Goddard AJH, Shaw G, Allen D (1994) Resuspension of monodisperse particles from short grass swards: a wind tunnel study. J Aerosol Sci 25(5):843–857. https://doi.org/10.1016/0021-8502(94)90051-5

Giess P, Goddard AJH, Shaw G (1997) Factors affecting particle resuspension from grass swards. J Aerosol Sci 28(7):1331–1349. https://doi.org/10.1016/S0021-8502(97)00021-9

Gu J, Pitz M, Schnelle-Kreis J, Diemer J, Reller A, Zimmermann R, Soentgen J, Stoelzel M, Wichmann H-E, Peters A, Cyrys J (2011) Source apportionment of ambient particles: comparison of positive matrix factorization analysis applied to particle size distribution and chemical composition data. Atmos Environ 45(10):1849–1857. https://doi.org/10.1016/j.atmosenv.2011.01.009

Hussein T, Hruška A, Dohányosová P, Džumbová L, Hemerka J, Kulmala M, Smolík J (2009a) Deposition rates on smooth surfaces and coagulation of aerosol particles inside a test chamber. Atmos Environ 43(4):905–914. https://doi.org/10.1016/j.atmosenv.2008.10.059

Hussein T, Kubincová L, Džumbová L, Hruška A, Dohányosová P, Hemerka J, Smolík J (2009b) Deposition of aerosol particles on rough surfaces inside a test chamber. Build Environ 44(10):2056–2063. https://doi.org/10.1016/j.buildenv.2009.02.009

Ibrahim AH, Dunn PF (2006) Effects of temporal flow acceleration on the detachment of microparticles from surfaces. J Aerosol Sci 37(10):1258–1266. https://doi.org/10.1016/j.jaerosci.2006.01.007

Ibrahim AH, Dunn PF, Brach RM (2003) Microparticle detachment from surfaces exposed to turbulent air flow: controlled experiments and modeling. J Aerosol Sci 34(6):765–782. https://doi.org/10.1016/S0021-8502(03)00031-4

Ibrahim AH, Dunn PF, Brach RM (2004) Microparticle detachment from surfaces exposed to turbulent air flow: effects of flow and particle deposition characteristics. J Aerosol Sci 35(7):805–821. https://doi.org/10.1016/j.jaerosci.2004.01.002

Ibrahim AH, Dunn PF, Qazi MF (2008) Experiments and validation of a model for microparticle detachment from a surface by turbulent air flow. J Aerosol Sci 39(8):645–656. https://doi.org/10.1016/j.jaerosci.2008.03.006

Kassab AS, Ugaz VM, King MD, Hassan YA (2013) High resolution study of micrometer particle detachment on different surfaces. Aerosol Sci Technol 47(4):351–360. https://doi.org/10.1080/02786826.2012.752789

Kim Y, Gidwani A, Wyslouzil BE, Sohn CW (2010) Source term models for fine particle resuspension from indoor surfaces. Build Environ 45(8):1854–1865. https://doi.org/10.1016/j.buildenv.2010.02.016

Lai ACK (2006) Investigation of electrostatic forces on particle deposition in a test chamber. Indoor Built Environ 15(2):179–186. https://doi.org/10.1177/1420326X06063219

Lai ACK, Nazaroff WW (2005) Supermicron particle deposition from turbulent chamber flow onto smooth and rough vertical surfaces. Atmos Environ 39(27):4893–4900. https://doi.org/10.1016/j.atmosenv.2005.04.036

Laidlaw MAS, Zahran S, Mielke HW, Taylor MP, Filippelli GM (2012) Re-Suspension of lead contaminated urban soil as a dominant source of atmospheric lead in birmingham, Chicago, Detroit and Pittsburgh, USA. Atmos Environ 49:302–310. https://doi.org/10.1016/j.atmosenv.2011.11.030

Laschober C, Limbeck A, Rendl J, Puxbaum H (2004) Particulate emissions from on-road vehicles in the Kaisermühlen- Tunnel (Vienna, Austria). Atmos Environ 38(14):2187–2195. https://doi.org/10.1016/j.atmosenv.2004.01.017

Lengweiler P, Nielsen PV, Moser A, Heiselberg P, Takai H (1998) Which parameters are important deposition and. Dept. of Building Technology and Structural Engineering. Indoor Environmental Engineering, No 92, Vol R9845

Li W, Ouyang Z, Zhou W, Chen Q (2011) Effects of spatial resolution of remotely sensed data on estimating urban impervious surfaces. J Environ Sci 23(8):1375–1383. https://doi.org/10.1016/S1001-0742(10)60541-4

Liu H, Weng Q (2013) Landscape metrics for analysing urbanization-induced land use and land cover changes. Geocarto Int 28(7):582–593. https://doi.org/10.1080/10106049.2012.752530

Lyu Y, Zhang K, Chai F, Cheng T, Yang Q, Zheng Z, Li X (2017) atmospheric size-resolved trace elements in a city affected by non-ferrous metal smelting: indications of respiratory deposition and health risk. Environ Pollut 224:559–571. https://doi.org/10.1016/j.envpol.2017.02.039

Maro D, Connan O, Hébert D, Rozet M (2008) Étude Du Dépôt Sec Des Aérosols En Milieu Urbain. 1:29–36

Martuzevicius D, Kliucininkas L, Prasauskas T, Krugly E, Kauneliene V, Strandberg B (2011) Resuspension of particulate matter and pahs from street dust. Atmos Environ 45(2):310–317. https://doi.org/10.1016/j.atmosenv.2010.10.026

Matsusaka S, Masuda H (1996) particle reentrainment from a fine powder layer in a turbulent air flow. Aerosol Sci Technol 24(2):69–84. https://doi.org/10.1080/02786829608965353

Mbengue S, Alleman LY, Flament P (2014) Size-distributed metallic elements in submicronic and ultrafine atmospheric particles from urban and industrial areas in Northern France. Atmos Res 135–136:35–47. https://doi.org/10.1016/j.atmosres.2013.08.010

Nicholson KW (1988) Review Article. Sciences (New York) 22(12):2639–2651

Nicholson KW (1993) Wind tunnel experiments on the resuspension of particulate material. Atmos Environ Part A 27(2):181–188. https://doi.org/10.1016/0960-1686(93)90349-4

Nicholson KW (2009) Chapter 2 The Dispersion, Deposition and Resuspension of Atmospheric Contamination in the Outdoor Urban Environment. Radioactivity in the Environment. Vol. 15. Elsevier. https://doi.org/10.1016/S1569-4860(09)00402-1

Ould-Dada Z, Baghini NM (2001) Resuspension of small particles from tree surfaces. Atmos Environ 35(22):3799–3809. https://doi.org/10.1016/S1352-2310(01)00161-3

Percot S (2012) Contribution des retombées Atmosphériques aux flux de polluants issus d'un petit bassin versant urbain: cas du Pin Sec à Nantes. Thèse de doctorat, École centrale de Nantes. tel-00851955

Qian J, Ferro AR (2008) Resuspension of dust particles in a chamber and associated environmental factors. Aerosol Sci Technol 42(7):566–578. https://doi.org/10.1080/02786820802220274

Qian J, Ferro AR, Fowler KR, Qian J, Ferro AR, Fowler Estimating KR, Qian J, Ferro AR, Fowler KR (2008) Estimating the resuspension rate and residence time of indoor particles estimating the resuspension rate and residence time of indoor particles. J Air Waste Manage Assoc 58(4):502–516. https://doi.org/10.3155/1047-3289.58.4.502

Reeks MW, Hall D (2001) Kinetic Models for Particle Resuspension in Turbulent Flows: Theory and Measurement. J Aerosol Sci 32:1–31. https://doi.org/10.1016/S0021-8502(00)00063-X

Richard A, Gianini MFD, Mohr C, Furger M, Bukowiecki N, Minguillon MC, Lienemann P, Flechsig U, Appel K, DeCarlo PF et al (2011) Source apportionment of size and time resolved trace elements and organic aerosols from an urban courtyard site in Switzerland. Atmos Chem Phys 11:8945–8963

Rosati JA, Thornburg J, Rodes C (2008) Resuspension of Particulate matter from carpet due to human activity. Aerosol Sci Technol 42(6):472–482. https://doi.org/10.1080/02786820802187069

Roupsard P (2013) Etude phénoménologique du d´dépôt sec d'aérosols en milieu urbain : Influence des propriétés des surfaces, de la turbulence et des conditions météorologiques. Thèse de doctorat, Rouen, INSA

Sabin LD, Lim JH, Venezia MT, Winer AM, Schiff KC, Stolzenbach KD (2006) Dry deposition and resuspension of particle-associated metals near a freeway in Los Angeles. Atmos Environ 40(39):7528–7538. https://doi.org/10.1016/j.atmosenv.2006.07.004

Sehmel GA (1980) Particle and gas dry deposition: a review. Atmos Environ (1967) 14(9):983–1011. https://doi.org/10.1016/0004-6981(80)90031-1

Sobhanardakani S (2018) Human health risk assessment of potentially toxic heavy metals in the atmospheric dust of city of Hamedan, West of Iran. Environ Sci Pollut Res 25(28):28086–28093. https://doi.org/10.1007/s11356-018-2818-0

Sobhanardakani S (2019) Ecological and human health risk assessment of heavy metal content of atmospheric dry deposition, a case study: Kermanshah, Iran. Biol Trace Elem Res 187(2):602–610. https://doi.org/10.1007/s12011-018-1383-1

Sternbeck J, Sjödin Å, Andréasson K (2002) Metal emissions from road traffic and the influence of resuspension - results from two tunnel studies. Atmos Environ 36(30):4735–4744. https://doi.org/10.1016/S1352-2310(02)00561-7

Thatcher TL, Layton DW (1995) I Nfiltrati. Atmos Environ 29(13):1487–1497

Thatcher TL, Fairchild WA, Nazaroff WW (1996) Particle deposition from natural convection enclosure flow onto smooth surfaces. Aerosol Sci Technol 25(4):359–374. https://doi.org/10.1080/02786829608965402

Thorpe A, Harrison RM (2008) Sources and properties of non-exhaust particulate matter from road traffic: a review. Sci Total Environ 400(1–3):270–282. https://doi.org/10.1016/j.scitotenv.2008.06.007

Thorpe AJ, Harrison RM, Boulter PG, McCrae IS (2007) estimation of particle resuspension source strength on a major London road. Atmos Environ 41(37):8007–8020. https://doi.org/10.1016/j.atmosenv.2007.07.006

Visser S, Slowik JG, Furger M, Zotter P, Bukowiecki N, Dressler R, Flechsig U, Appel K, Green DC, Tremper AH, Young DE, Williams PI, Allan JD, Herndon SC, Williams LR, Mohr C, Xu L, Ng NL, Detournay A, Barlow JF, Halios CH, Fleming ZL, Baltensperger U, Prévôt ASH (2015) Kerb and urban increment of highly time-resolved trace elements in PM10, PM2.5 and PM1.0 winter aerosol in London during ClearfLo 2012. Atmos Chem Phys 15(5):2367–2386. https://doi.org/10.5194/acp-15-2367-2015

Weinbruch S, Worringen A, Ebert M, Scheuvens D, Kandler K, Pfeffer U, Bruckmann P (2014) A quantitative estimation of the exhaust, abrasion and resuspension components of particulate traffic emissions using electron microscopy. Atmos Environ 99:175–182. https://doi.org/10.1016/j.atmosenv.2014.09.075

Wu YL, Russell AG (1992) Controlled wind tunnel experiments for particle bounceoff and resuspension. Aerosol Sci Technol 17(4):245–262. https://doi.org/10.1080/02786829208959574

Acknowledgements

Special thanks to the members of the Water and Environment laboratory, Nadège Caubrière, Martin Guillon and Dominique Demare, for their precious help during the analyses.